JOURNAL OF GEOPHYSICAL RESEARCH, VOL. 111, D15206, doi:10.1029/2005JD006890, 2006

Multiyear Advanced Very High Resolution Radiometer observations of summertime stratocumulus collocated with aerosols in the northeastern Atlantic

Mark A. Matheson,[1,2] James A. Coakley Jr.,[1] and William R. Tahnk[1]

Received 15 November 2005; revised 18 April 2006; accepted 26 April 2006; published 8 August 2006.

[1] Advanced Very High Resolution Radiometer (AVHRR) 4-km data were collected over the northeast Atlantic for May–August 1995–1999. Aerosol optical depth at 0.55 μm was retrieved in pixels identified as being cloud-free ocean. In pixels identified as containing clouds from single-layered, low-level cloud systems over oceans, the following cloud properties were retrieved: 0.64-μm cloud optical depth, droplet effective radius, cloud layer altitude, pixel-scale fractional cloud cover, column liquid water amount and column droplet concentration. Aerosol and cloud properties were averaged in 1° × 1° latitude-longitude regions. Regions that contained clouds were limited to those in which all the clouds were part of a single-layered, low-level cloud system. Aerosol and cloud properties were compared only in 1° regions that had sufficient numbers of both cloud-free pixels that yielded aerosol retrievals and cloudy pixels that yielded retrievals of cloud properties within a single overpass. The comparisons were collected in 5° × 5° latitude-longitude regions to determine trends. Within each 5° region the cloud properties were similar from year to year, permitting the data to be composited for all 5 years. Aerosol optical depth decreased systematically with time, probably as a result of the increase in solar zenith angle due to the precession of the satellite orbit. Within the 5° regions, as aerosol optical depth increased, droplet effective radius decreased, cloud optical depth increased, and droplet column number concentration increased, qualitatively consistent with the trends expected for the aerosol indirect effect. In some regions, liquid water path decreased as aerosol optical depth increased, contrary to the trends expected for the suppression of drizzle. Within each 5° region, clouds in clean air, as indicated by their collocation with relatively small aerosol optical depths, had larger droplets and smaller cloud optical depths than clouds in polluted air, as indicated by their collocation with relatively large aerosol optical depths. On average, the aerosol indirect radiative forcing for overcast conditions was about twice as large as the direct radiative forcing for cloud-free conditions. In most of the 5° regions increases in cloud liquid water with increasing aerosol optical depth enhanced the ratios by 20–30% over those calculated from the changes in droplet effective radius and an assumption of constant cloud liquid water. In some 5° regions, however, like those just to the west of the Iberian peninsula, the column amount of cloud liquid water decreased with increasing aerosol optical depth.

Citation: Matheson, M. A., J. A. Coakley Jr., and W. R. Tahnk (2006), Multiyear Advanced Very High Resolution Radiometer observations of summertime stratocumulus collocated with aerosols in the northeastern Atlantic, *J. Geophys. Res.*, *111*, D15206, doi:10.1029/2005JD006890.

1. Introduction

[2] Seeking evidence for aerosol indirect radiative forcing and using observations to empirically derive estimates of the forcing has proven elusive. In a previous paper [*Matheson et al.*, 2005, hereinafter referred to as MCT], NOAA 14 4-km Advanced Very High Resolution Radiometer (AVHRR) data were used to determine the response of the 1995 summertime marine stratocumulus in the northeastern Atlantic to variations in aerosol loading. As MCT noted, signs of the effects of the aerosols on the clouds, namely the decrease in droplet radius, the increase in visible optical depth, and the increase in column droplet number concentration, were consistent with what has become known as the "Twomey Effect" [*Twomey*, 1974]. The findings were qualitatively consistent with many of the findings of other studies in which regional and even global-scale cloud and aerosol

[1] College of Oceanic and Atmospheric Sciences, Oregon State University, Corvallis, Oregon, USA.
[2] Now at Building Research Institute, Department of Environmental Engineering, Tsukuba, Japan.

0148-0227/06/2005JD006890$09.00

properties were similarly associated in attempts to estimate the aerosol indirect radiative forcing [*Kaufman and Nakajima*, 1993; *Kaufman and Fraser*, 1997; *Wetzel and Stowe*, 1999; *Nakajima et al.*, 2001; *Sekiguchi et al.*, 2003; *Quaas et al.*, 2004]. However, as MCT also noted, correlations of cloud properties with measures of aerosol concentrations are unlikely to determine the effects of the particles on the clouds. MCT listed a host of physical processes that are likely to affect aerosols and the retrieval of aerosol properties in the vicinity of clouds as well as affect the cloud properties. MCT also found that the low-level marine clouds near the European continent appeared to lose liquid water as the aerosol burden rose, in contrast to global climate model predictions of the aerosol indirect forcing which indicate that cloud liquid water increases in polluted clouds and that this increase has a substantial impact on estimates of the forcing [*Lohmann et al.*, 2000; *Lohmann and Lesins*, 2002]. The loss in liquid water might be explained by the drying of the clouds and boundary layer through the enhanced entrainment in the polluted clouds of dry continental air overlying the marine boundary layer [*Ackerman et al.*, 2004]. *Harshvardhan et al.* [2002] also noted the competition between the response of the clouds to aerosols and their response to the thermodynamics of their environment.

[3] In addition, MCT found that as regional cloud cover fraction increased, cloud optical depth and droplet effective radius also increased. They interpreted these trends as a manifestation of intrinsic relationships among the cloud properties. As a region becomes heavily cloud covered, the clouds thicken. In adiabatic cloud parcel models, cloud optical depth and droplet radius increase as the geometric thickness of the clouds increases [*Brenguier et al.*, 2000; *Szczodrak et al.*, 2001]. At the same time, the retrieved aerosol optical depth also increased as the regional cloud cover increased; yet, when the aerosol optical depth was correlated with droplet effective radius, the droplet radius decreased as the aerosol optical depth increased. The increases in aerosol optical depth and droplet radius with fractional cloud cover and the simultaneous decrease in droplet radius with increasing aerosol optical depth were explained in terms of the widely dispersed distributions exhibited by the cloud properties. Within each increment of aerosol optical depth, clouds with a wide range of properties coexisted with the aerosol. The trend in the mean of those properties was toward clouds with smaller droplets when the aerosol optical depth was high. Given the large dispersions of the cloud properties associated with a particular aerosol optical depth, such trends might have been influenced by statistical sampling errors. Such errors are reduced by increasing the number of statistically independent cases used in the analysis.

[4] Here, the number of cases included in the analysis is expanded by incorporating the summertime observations for 5 years (1995–1999) of NOAA 14 AVHRR observations. The cloud properties and aerosol optical depths for the 5-year period were examined to determine year-to-year variations. The regional-scale year-to-year variations proved to be small compared with estimates of the statistical uncertainty in the means of the cloud properties and substantially smaller than the daily variability that these properties exhibited within each region studied (section 2). The similarity of the cloud properties and aerosol optical depths throughout the period justified the grouping of all observations into a single ensemble. The trends reported in MCT were then examined for their stability in the face of the larger ensemble of cases (section 3). The larger ensemble also allowed the separation of cloud data into those that occurred on relatively unpolluted "clean" days and those that occurred on relatively "polluted" days. This separation revealed changes in the cloud properties associated with small and large aerosol burdens regardless of the regional cloud cover which, as noted by MCT, affect both the cloud droplet effective radius and visible optical depth. Changes in cloud properties derived from the clean and polluted days were then used to calculate the ratio of the aerosol indirect radiative forcing for overcast conditions to that for the direct radiative forcing for cloud-free conditions. These estimates of the radiative forcing were compared with those derived using the trends in cloud properties with aerosol optical depth, as was done in MCT and in many of the earlier studies (section 4).

2. Data and Methodology

[5] Global Area Coverage (GAC) radiances from the NOAA 14 AVHRR were analyzed for all daytime passes over the northeastern Atlantic during May through August for the years 1995–1999. The region of analysis was bounded by 35–55°N latitude and 0–20°W longitude. Pixels over land were not used. NCEP reanalysis data showed periods of sustained onshore and offshore flow which gave rise to a wide range of aerosol burdens mixing with the marine stratus and stratocumulus that were frequently found in this region during the summer.

[6] The analysis methodology was described in MCT and is summarized briefly here. The shortwave reflectivities for the NOAA 14 AVHRR were calibrated following *Tahnk and Coakley* [2001a, 2001b] and the 3.7 and 11-μm radiances were calibrated using standard methods [*Kidwell*, 1995]. Pixels within 40° of the sun's reflection, assuming specular reflection from a flat surface, were assumed to have been affected by sun glint and were removed from further analysis. A scene identification scheme was used to identify 4-km pixels as cloud-free, partially covered by clouds, completely overcast by clouds in a single layer, or overcast by clouds distributed in altitude. For cloud-free pixels, a two-channel scheme developed for retrieving aerosol properties for the Indian Ocean Experiment (INDOEX) was used to retrieve the 0.55-μm aerosol optical depth and apportion the fraction of the optical depth associated with a marine aerosol, which was made up of large nonabsorbing particles, and an average continental aerosol, which was made up of small absorbing particles [*Coakley et al.*, 2002]. The aerosol models are described by *Hess et al.* [1998]. Following *Coakley et al.* [2005], for pixels that contained clouds that were part of a single-layered, low-level system, a partly cloudy pixel retrieval scheme was used to obtain the 0.64-μm cloud optical depth, τ_c, droplet effective radius, R_e, cloud top altitude, and pixel-scale fractional cloud cover. In turn, these retrieved properties were used to derive cloud liquid water path, which was taken to be given by $W = \frac{2}{3} R_e \tau_c \rho$, where ρ = 1 g cm^{-3} is the density of water, and column droplet concentration, which was taken to be given by $N_c = \frac{\tau_c}{2\pi R_e^2}$.

[7] There are two steps in analyzing the retrieved aerosol and cloud properties. First, 1° × 1° latitude-longitude regions were selected for analysis only if they contained both cloudy pixels that yielded retrievals of cloud properties and cloud-free pixels that yielded retrievals of the aerosol properties. This requirement ensured that the cloud and aerosols were collocated at the time of the overpass. As was noted in MCT, the autocorrelation length of aerosol optical depth is order 100 km thereby allowing the assumption that aerosols found in a 1° region were probably similar to aerosols commingled with the clouds in the same region. Implicit in this assumption is that the clouds and aerosols are collocated within the same atmospheric layer. Determining that the aerosols and clouds occupy the same layer awaits observations like those hoped for with the CALIPSO lidar as part of the A-Train suite of instrumentation. With regard to the clouds in the 1° region, as discussed below, all the clouds had to be part of a single-layered, low-level marine stratocumulus system.

[8] The second step of the analysis was the collection of the 1° regional average aerosol and cloud properties for the individual passes in the corresponding 5° × 5° latitude-longitude region. Relationships between aerosol optical depth and cloud properties were then constructed on the basis of the observations that fell within each 5° region. The grouping into 5° regions was motivated by a desire to keep the cloud and aerosol properties as homogeneous as possible within each region so that the relationship between the cloud properties and aerosol optical depth would depend neither on the location of the 1° region within the 5° region nor the day on which the observation was made. Clouds, of course, are affected by the thermodynamics of their environment. By collecting a large number of collocated cloud and aerosol observations, the breadth of cloud and aerosol properties in each 5° region might be sampled. Provided that the aerosol properties are unrelated to the thermodynamic structure of the atmosphere that affects the cloud properties, the effects of the aerosols on the clouds might be deduced from the trends of the cloud properties with aerosol burdens. The assumption is that for a relatively homogeneous ensemble of clouds, the effects of the thermodynamic environment on the averages of the cloud properties would become small for a sufficiently large ensemble of observations. Unfortunately, known physical processes limit the validity of this assumption. First, *Platnick and Twomey* [1994] found that the response of the clouds to added particles depended on the properties of the clouds, which in turn, presumably depend on the thermodynamics of the cloud environment. Second, as was found for the 1995 observations in MCT, large aerosol optical depths appeared to be linked to dry continental air, particularly for the regions near the European coast. There the clouds probably respond not only to the aerosols but also to the dryness of the air accompanying the aerosol. As MCT noted, the breakup of the analysis into 5° regions was also undertaken to avoid spurious relationships that could arise from the geographic distributions of the cloud and aerosol properties, such as the gradients in aerosol burdens and cloud properties found near the European coast. Similar gradients off the coast of southern California were noted and addressed by *Shao and Liu* [2005].

[9] Aerosol retrievals were performed for the cloud-free pixels and cloud property retrievals were performed for the cloudy pixels and the pixel-scale results for each satellite pass were mapped into 1° regions. The 1° regions were limited to those in which all clouds were part of a low-level, single-layered cloud system. Such regions were identified by (1) the lack of low values for pixel-scale emission at 11 μm and (2) for the 1° regions that contained overcast pixels, the temperatures retrieved for the cloud layers in the region had the following properties: (1) They were consistent with the lowest pixel-scale 11-μm emission and (2) they had a standard deviation that was substantially smaller than the difference between the average surface and cloud layer temperatures within the region, thereby indicating the presence of a well-defined cloud layer. Regions with upper level clouds or multilayered cloud systems were avoided because of the potential for contamination of the properties retrieved for the low-level, single-layered clouds. Details of the cloud screening are described in MCT. The mean of all cloud and aerosol properties were calculated for each satellite overpass for each 1° region. For the cloud properties, the pixel-scale values, including cloud liquid water path and column droplet concentration, were weighted by the pixel-scale fractional cloud cover to calculate the 1° regional overpass means. For the aerosol optical depths, the means of the fine mode optical depth, associated with the continental aerosol, the coarse mode optical depth, associated with the marine aerosol, and the total optical depth, which is the sum of the fine and coarse mode optical depths, were calculated. To ensure that representative means for the region were obtained and that the region contained both clouds and aerosols, a minimum of 10 pixels or 5% of all pixels in the 1° region, whichever was larger, was required for both the cloud-free pixels that yielded aerosol properties and the cloudy pixels that yielded cloud properties for the region.

[10] The observations for the 1° regions were gathered into 5° regions for individual years and the 5th and 95th percentiles of the overpass 1° regional means for all cloud and aerosol properties were calculated for each year. With the exception of fractional cloud cover, if the mean value of an aerosol or cloud property for a 1° region from a single satellite overpass was outside the 5th and 95th percentiles for a particular year and 5° region, that overpass 1° regional mean was considered to be an outlier and all aerosol and cloud properties for that 1° region and overpass were eliminated. Fractional cloud cover ranges from values near zero to values near unity, so extremes in fractional cloud cover were not considered outliers.

[11] Figure 1 shows the standard deviations of the passes within the years (outer range of error bars), and standard errors (inner range of error bars) for the 0.55-μm aerosol optical depth and selected cloud properties in each 5° region for each of the 5 years. The standard errors were taken to be given by the standard deviation of the individual pass means divided by the square root of the number of satellite overpasses. They serve as estimates of the statistical uncertainty in the means. The means of the quantities lie midway between the inner error bars associated with the standard errors. Clearly, the variability of the quantities within each year is substantially larger than the year-to-year variability in the means. While the yearly averages of droplet effective radius, cloud optical depth, and fractional cloud cover

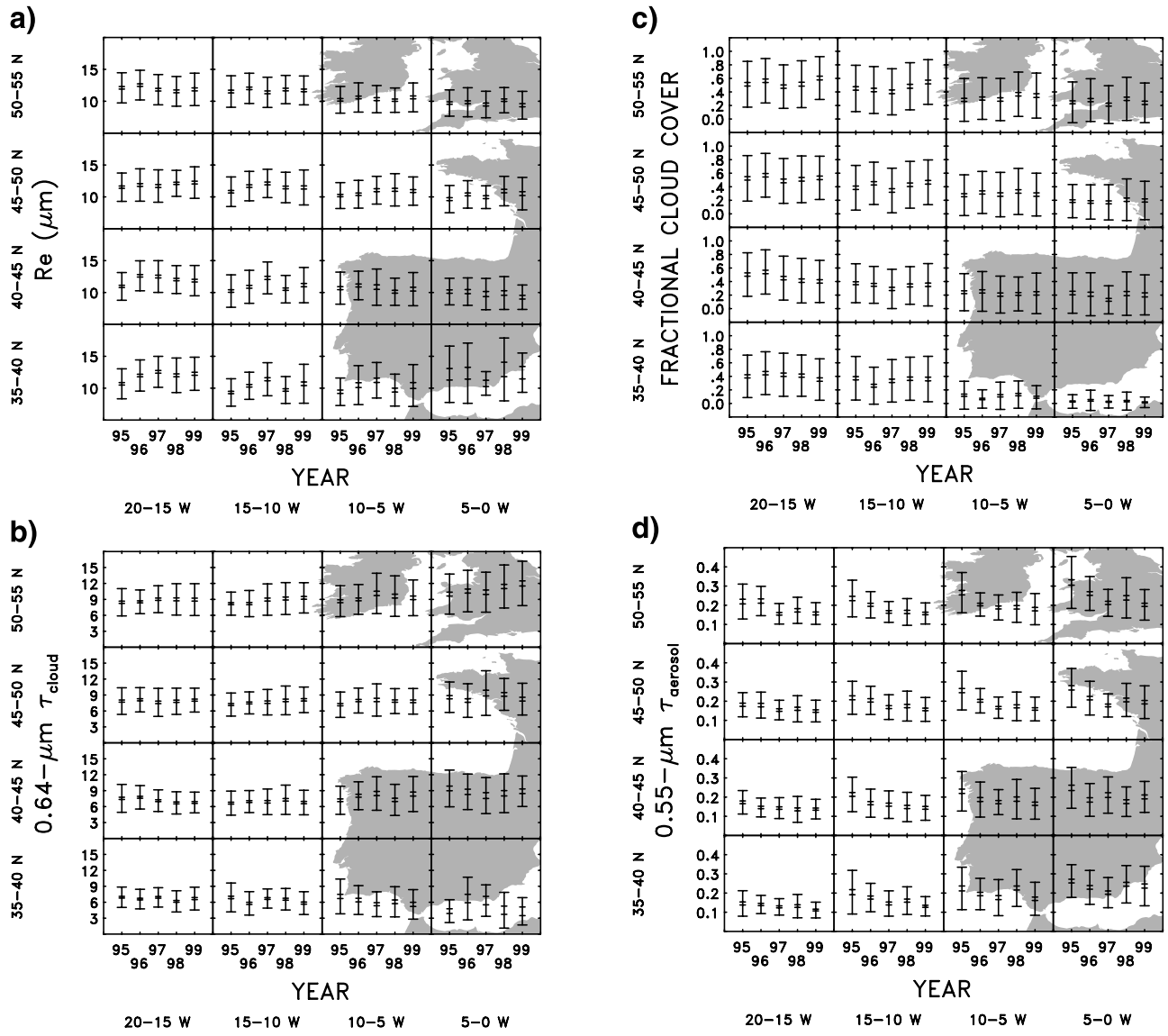

Figure 1. Standard deviation (outer range of error bars) and standard error (inner range of error bars) for (a) droplet effective radius (μm), (b) 0.64-μm cloud optical depth, (c) fractional cloud cover, and (d) 0.55-μm aerosol optical depth. The standard error is given by the standard deviation divided by the square root of the number of samples, in this case, the number of satellite overpasses that contributed observations. All cloud properties are for single-layered, low-level clouds. Means were calculated for every daytime satellite overpass in $1° \times 1°$ latitude-longitude regions. In calculating the pass averages within a region, cloud properties were weighted by the pixel-scale fractional cloud cover. These pass means were then averaged for May–August in the $5° \times 5°$ latitude-longitude regions. Data from individual years, 1995–1999, are shown in their respective 5° region.

fluctuated about their 5-year mean values, the fluctuations were small, often smaller than the standard errors estimated for the yearly means.

[12] Only aerosol optical depth showed a trend toward smaller values as time progressed. The retrieved aerosol optical depth decreased as the solar zenith angle of the observations increased, from an average of 34° for the observations in 1995 to 47° in 1999. The increase in solar zenith angle was caused by the shift to later equator crossing times of the NOAA 14 orbit. A similar decrease in aerosol optical depth due to a shift in the orbit of NOAA 9 was reported by *Stowe et al.* [2002]. Of course, some of the decrease in aerosol optical depth might also arise from errors in the calibration of the AVHRR shortwave reflectivities, which are expected to be within 5% [*Tahnk and Coakley*, 2001a, 2001b]. That similar trends were not found for the retrieved cloud optical depths suggests that the calibration errors were not a major factor in the aerosol optical depth trends, although the variability in cloud optical depths would all but mask the effects of a 5% error in calibration. In any case, as discussed below and in section 3, trends in cloud properties with aerosol optical depths were derived from the daily variability of the cloud properties and aerosol optical depths for the 5 year period. Despite the

Table 1. Number and Percentage of 1° × 1° Latitude-Longitude Regions That Survived Successive Data Screening Tests[a]

Screening	Aerosol		Cloud	
	Number	%	Number	%
At least 10 pixels or 5% (whichever was greater) of all pixels in region had either cloud or aerosol retrievals	59,063	21.8	131,541	48.5
Region contained only cloud-free pixels or clouds from single-layered, low-level cloud systems	47,745	17.6	70,641	26.0
Region contained cloud and aerosol properties that were within the 5th and 95th percentile for that 5° region	39,579	14.6	47,714	17.6
Region contained both cloud and aerosol retrievals that passed previous data screening tests	9,247	3.4	9,247	3.4

[a]Percentages are based on 271,301 1° regions from 2499 satellite overpasses that contained at least one pixel that was observed during daytime, over water, and away from sun glint and was therefore suitable for attempting cloud and aerosol retrievals.

decrease in aerosol optical depth with time, its daily variability remained about the same within many of the regions over the 5 year period.

[13] Because of the year-to-year consistency in the averages and standard deviations of the cloud and aerosol properties within each of the 5° regions, all 5 years of data were composited into a single ensemble of observations. Hereinafter, the removal of outlier data was performed by calculating the 5th and 95th percentiles on the basis of the 5-year composite of data within each of the 5° regions rather than on individual years as was done for the analysis presented in Figure 1.

[14] Table 1 gives the number of 1° regions for which retrievals were attempted and the reduction in the numbers that resulted from the application of each of the screening rules. Cloud or aerosol retrievals were attempted in a total of 271,301 1° regions that contained pixels that were observed during daytime, away from sun glint, and over water. Only 3.4% of the candidate regions passed the screening process that ensured that all clouds in the region were part of a single-layered system and the region had sufficient numbers of both cloud and aerosol retrievals to enable a comparison of cloud and aerosol properties. This percentage of usable 1° regions is similar to the 2.9% found for 1995 (MCT). The 5 years of data provided 5.3 times the number of samples used in MCT, thereby facilitating analyses that could not be performed with the 1995 observations alone and also providing greater statistical confidence in the results.

[15] Figure 2 shows the geographical distributions for aerosol optical depth, droplet effective radius, cloud optical depth, and cloud cover fraction. The data in each satellite overpass were averaged in 1° regions and then all overpass means in that 1° region were averaged over the 5 years to produce the climatology. The climatology was constructed only from 1° regions which met the criteria ensuring that the clouds within the region were part of a single-layered, low-level system. Unlike the results presented in Figure 1, in Figure 2, 1° regions that were completely overcast by single-layered, low-level clouds and regions that were completely cloud-free were included. Smoothing was applied to the mean values for the 1° regions to emphasize the large-scale trends.

[16] The geographical distributions shown in Figure 2 are similar to those found for 1995 in MCT. During the summer months of 1995–1999, aerosol optical depth was, on average, highest near the coast (Figure 2a). Cloud droplet effective radii were smallest and cloud optical depths were largest near the coast (Figures 2b and 2c). That regions with larger aerosol optical depths had smaller droplet radii and larger cloud optical depths might be a manifestation of the Twomey Effect. On the other hand, it is possible that air flowing off the continent was more polluted and dryer than marine air at the same location. Continental air may have given rise to a drying of the clouds and marine boundary layer leading to smaller cloud droplets and cloud fractions near the coast (Figure 2d). Because cloud liquid water amount is proportional to the product of droplet radius and optical depth, clouds can undergo a decrease in cloud liquid water due to a decrease in droplet radius, as happens to the west of the Iberian peninsula, even though the optical depth increases. Clearly, the observations embrace a mix of processes. Clouds may be responding to the thermodynamics of the environment in which they are imbedded as well as to the aerosol burden.

3. Collocated Aerosol Optical Depths and Cloud Properties

[17] Figures 3–5 show various properties of low-level, single-layered clouds associated with aerosol optical depth. For each satellite overpass, the mean of the aerosol optical depth and all cloud properties were calculated for 1° regions. As mentioned in section 2, all clouds within the 1° region had to be part of a single-layered, low-level cloud system for the region to be included in the analysis. In addition, the region had to contain sufficient numbers of pixels yielding retrievals of cloud properties and aerosols so that the mean properties were representative of a regional average. Cloud properties were associated only with aerosol optical depths from the same 1° region for the same satellite overpass. The 1° regional average cloud properties and aerosol optical depths were then composited in the associated 5° region. This compositing was used to increase the sample size within each of the 5° regions. Smaller regions would have been preferable to achieve a higher degree of homogeneity in cloud and aerosol properties in the face of the geographic trends evident in Figure 2. Unfortunately, even at the 5° regional scale, the number of cases was sometimes insufficient to achieve high levels of statistical confidence in the trends.

[18] The cloud properties in each 5° region were composited into the associated 0.05 wide bins of the 0.55-μm aerosol optical depth. The mean and standard error of the overpass means were calculated for each aerosol bin. Bins with overpass means from fewer than 10 separate satellite overpasses were excluded. The slope and standard deviation of the slope were estimated from a linear fit to the bin means

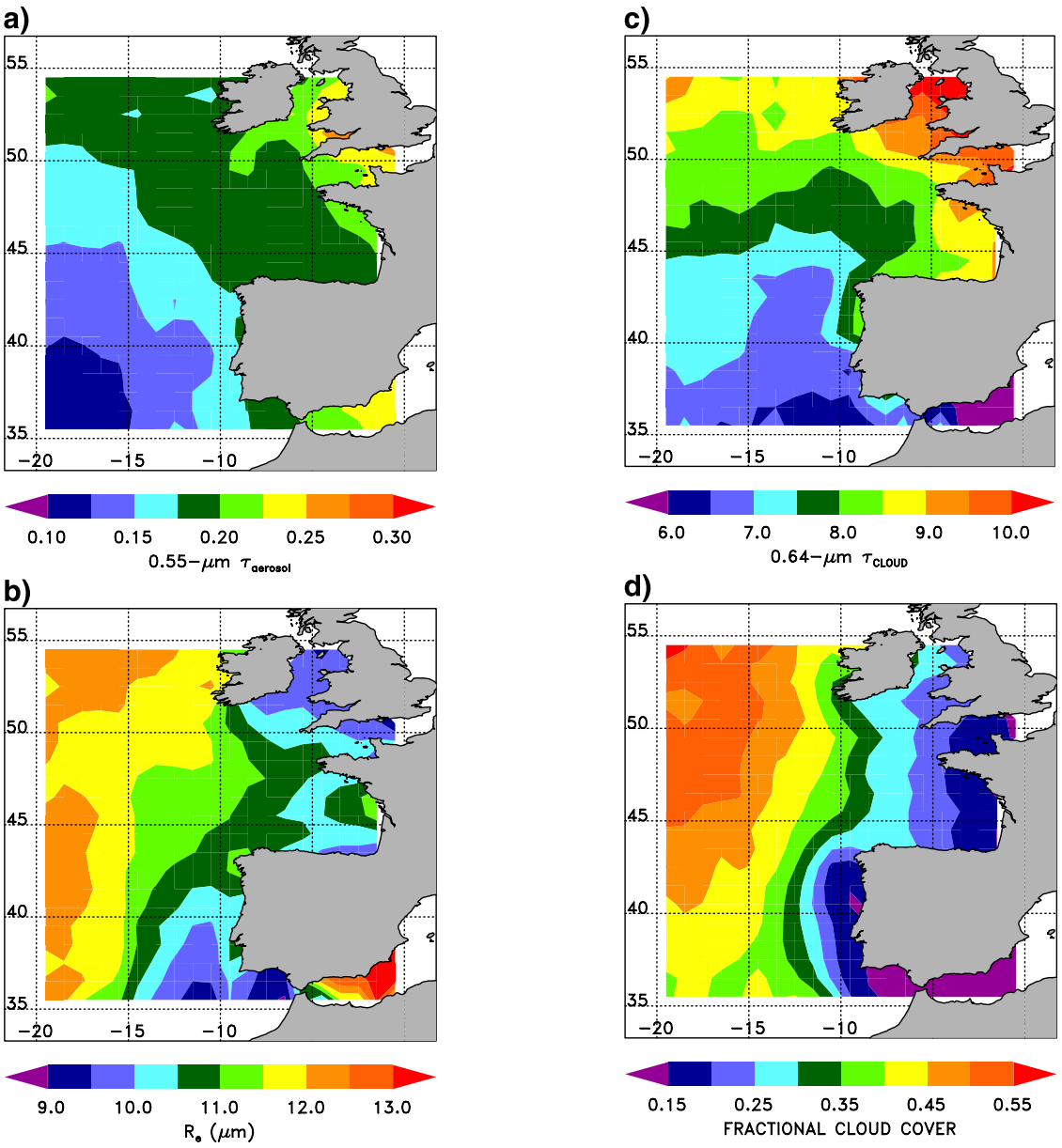

Figure 2. Mean properties of single-layered, low-level clouds and 0.55-μm aerosol optical depth for May–August 1995–1999: (a) 0.55-μm aerosol optical depth, (b) droplet effective radius (μm), (c) 0.64-μm cloud optical depth, and (d) fractional cloud cover. The contours have been smoothed to show the large-scale trends. The aerosol optical depths were from 1° regions that were either cloud-free or in which all of the clouds in the region were part of a single-layered, low-level system. The cloud properties were from 1° regions in which all of the clouds were part of a single-layered, low-level cloud system. Regions that were overcast by single-layered, low-level clouds were also included. In calculating the overpass regional averages, pixel-scale cloud properties were weighted by the pixel-scale fractional cloud cover.

weighted by the inverse of the standard errors of the bin means [*Bevington*, 1969]. 5° regions with bin means from fewer than five aerosol optical depth bins were considered to have insufficient data for calculating trends and were left blank in the figures.

[19] As was done in MCT, the cloud properties in Figures 3–5 were correlated with the total aerosol optical depth, as opposed to the fine or coarse mode optical depths, as the total optical depth had the greatest correlation with the cloud properties. As most of the aerosol was in the fine mode, associated with an average continental aerosol, the total optical depth was well correlated with the fine mode optical depth. Neither the total optical depth nor the cloud properties were well correlated with the coarse mode optical depth. Nonetheless, when significant trends were obtained with both the total and coarse mode optical depths, as for example, changes in cloud optical depth with aerosol optical depth, the changes were in the same direction with the exception of one 5° region for the correlation between cloud altitude and aerosol optical depth.

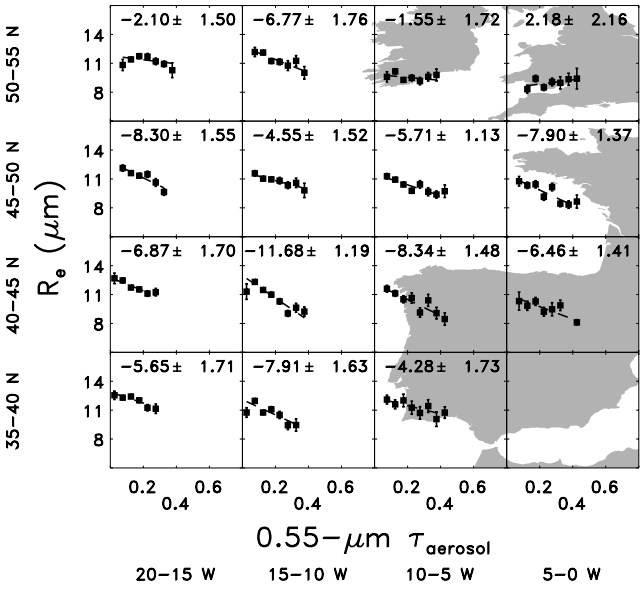

Figure 3. Means of overpass averaged droplet effective radius (μm) for 1° regions binned for each 0.05 interval of aerosol optical depth. Each panel contains data from that 5° region. Error bars represent the standard error, given by the standard deviation of the means from individual passes for that bin divided by the square root of the number of passes that contributed observations to that bin. The dashed line is a linear fit to the bin means inversely weighted by the standard error. Also given are the mean and standard error estimated for the slope of the linear fit.

[20] In most of the 5° regions, droplet effective radius decreased as aerosol optical depth increased (Figure 3). Similar trends were found in MCT, but the greater number of cases contributed by the multiyear observations allowed for an investigation of additional 5° regions surrounding the Iberian Peninsula and also larger ranges of aerosol optical depth in many of the regions. Cloud optical depth (Figure 4) increased with increasing aerosol optical depth in the majority of the 5° regions. Because column droplet number concentrations are proportional to the cloud optical depth and inversely proportional to the square of the droplet effective radius, the droplet numbers increased with increasing aerosol optical depth in all regions (not shown), as might be inferred from the trends in droplet effective radii (Figure 3) and cloud optical depths (Figure 4). Cloud altitude stayed constant with changing aerosol optical depth in many regions but tended to decrease as aerosol burden increased around the Iberian Peninsula (not shown).

[21] Twomey's original estimates of the aerosol indirect radiative forcing invoked fixed cloud liquid water amounts [*Twomey*, 1974]. *Albrecht* [1989] suggested that cloud liquid water would increase with increasing aerosol burden owing to the suppression of drizzle. In six of the fifteen 5° regions, the slope of the change in liquid water amount with aerosol optical depth was greater than twice the estimated error, thereby indicating statistically significant trends (Figure 5). Five of the six regions exhibited a decrease in cloud liquid water as aerosol burden increased. Air masses with larger aerosol burdens probably originated over the continent and were therefore dryer than less polluted, oceanic air masses. *Ackerman et al.* [2004] suggest that when the air in the free troposphere above the clouds is sufficiently dry, polluted clouds should lose liquid water as appears to occur near the coast in the results shown in Figure 5.

[22] The results shown in Figures 3–5 are consistent with the Twomey Effect. Clouds in regions with larger aerosol burdens had larger column droplet concentrations, smaller droplets and larger optical depths. Nonetheless, cloud properties are highly variable, and changes in cloud properties may arise from factors other than the effects of aerosols. As was noted in MCT and as is shown in Figure 6, aerosol optical depth appeared to increase as the percentage of cloudy pixels within a 1° region increased in most of the 5° regions. This increase in aerosol optical depth could have

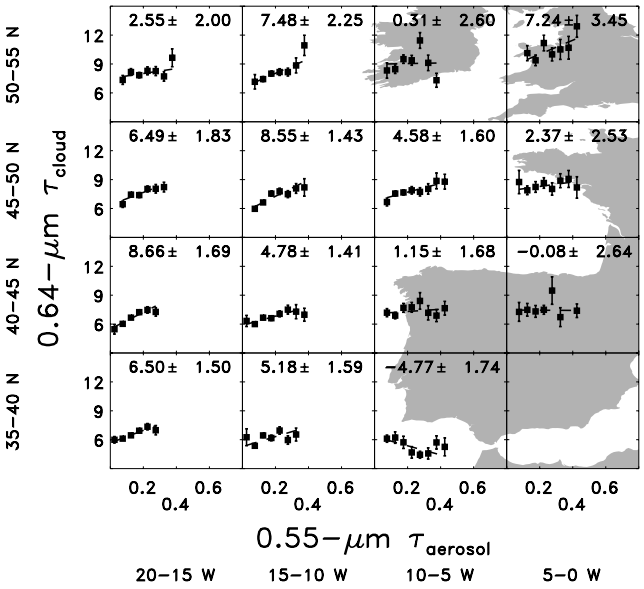

Figure 4. Same as Figure 3 but for 0.64-μm cloud optical depth.

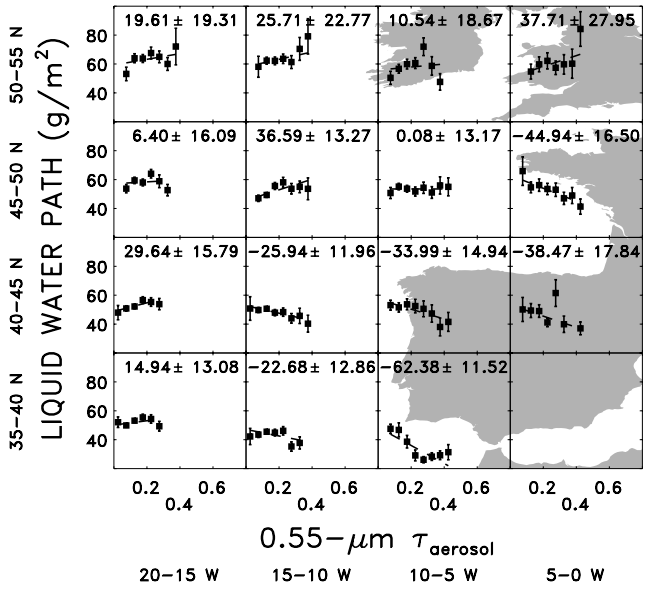

Figure 5. Same as Figure 3 but for liquid water path (g/m^2).

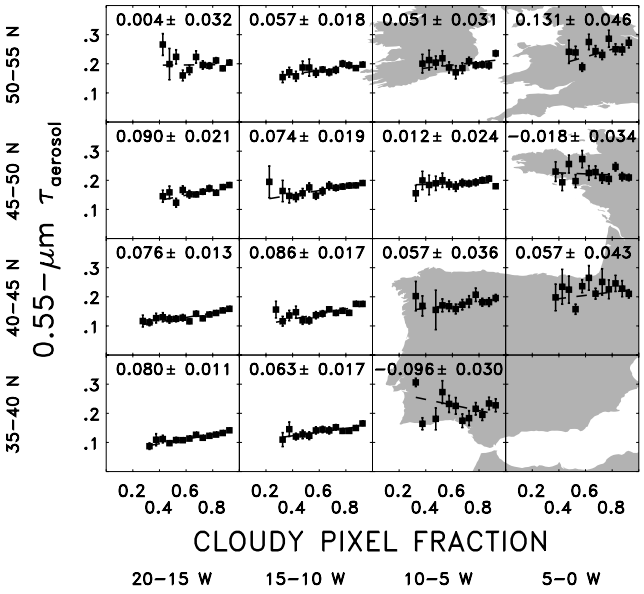

Figure 6. Same as Figure 3 but for 0.55-μm aerosol optical depth and cloudy pixel fraction. Cloudy pixel fraction is the fraction of pixels within a 1° region identified as containing clouds (pixel-scale cloud fraction > 0.2). Only regions that contained a sufficient number of cloud retrievals for which the properties are presented in Figures 3–5 were included.

been caused by cloud contamination in the cloud-free pixels used to retrieve the aerosol properties. Undetected subpixel-scale clouds in the cloud-free pixels cause the retrieved aerosol optical depths to be erroneously high. As cloud fraction increases, the degree of cloud contamination is likely to increase. In addition to cloud contamination, the increase in aerosol optical depth could have resulted from the swelling of aerosol particles in the higher humidity cloud environment [*Seinfeld and Pandis*, 1998; *Clarke et al.*, 2002]. Increased particle production near clouds [*Kütz and Dubois*, 1997] and an increase in aerosol size caused by in-cloud processing [*Lelieveld and Heintzenberg*, 1992] are also possible explanations for the increase in aerosol optical depth near clouds. Likewise, sunlight reflected by nearby clouds enhances the illumination of the adjacent cloud-free pixels thereby causing the aerosol optical depth to be overestimated [*Podgorny*, 2003]. As MCT noted, with both aerosol and cloud optical depths increasing with increasing cloud cover, the apparent correlation between cloud and aerosol optical depths (Figure 4) cannot be solely the result of the Twomey Effect. The changes in retrieved aerosol and cloud properties may arise from changes in the cloud environment that affect both cloud and aerosol properties as well as fractional cloud cover.

[23] In an attempt to identify changes in cloud properties attributable to changes in aerosol burden, the cloud properties were divided into two sets, one that included 1° regions with mean 0.55-μm aerosol optical depths less than 0.13, the 40th percentile of aerosol optical depths for the entire 20° latitude-longitude domain, and a second that contained 1° regions with aerosol optical depths greater than 0.17, the 60th percentile of the aerosol optical depths. For convenience, these two sets will be referred to as "clean" and "polluted" clouds. Cloud properties associated with the midrange of aerosol optical depths were excluded from this analysis. Figures 7–9 show the trends in cloud properties binned for each 0.05 increment in the 1° regional cloud cover for both the clean (circles) and polluted clouds (crosses). Bin means are shown only for bins that had at least ten samples. Trends were not calculated in regions with fewer than five of the fractional cloud cover bins occupied by either the clean or polluted cloud ensembles. In such regions, the number of cases was judged to be insufficient for establishing a reliable trend.

[24] Droplet effective radius increased as fractional cloud cover increased for both the clean clouds (circles in Figure 7) and the polluted clouds (crosses) indicating that at least some of the observed changes in droplet radius were due to factors that affected cloud cover. Nonetheless, with the exception of one of the 5° regions, the clean clouds had larger droplets than the polluted clouds, regardless of regional cloud cover, indicating that some of the change in droplet size could be associated with changes in aerosol burden.

[25] In the fifteen 5° regions which had observations sufficient to calculate trends in cloud optical depths with regional cloud cover for the 1995 observations, MCT

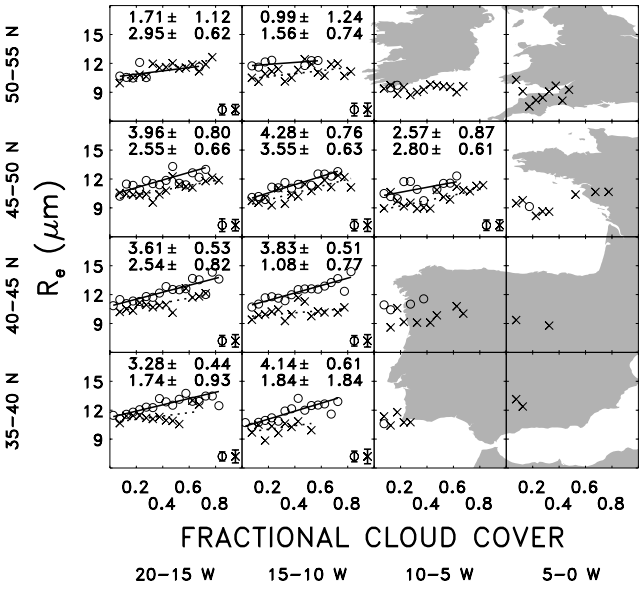

Figure 7. Means of overpass averaged droplet effective radius (μm) for 1° regions binned for each 0.05 interval of fractional cloud cover. Circles, representing clean clouds, are for 1° regions that had a mean aerosol optical depth less than 0.13, the 40th percentile of aerosol optical depths of all 1° regions within the 20° domain. Crosses, representing polluted clouds, are for 1° regions that had a mean aerosol optical depth greater than 0.17, the 60th percentile of aerosol optical depths. Error bars plotted in the lower right corner are the RMS of the standard error for the data points. The solid (dashed) line is a linear fit to the bin means of the clean clouds, indicated by circles (polluted clouds, indicate by crosses) inversely weighted by the standard error. Also given are the mean and standard error estimated for the slope of the linear fits for the clean (circles, top) and polluted (crosses, bottom) clouds.

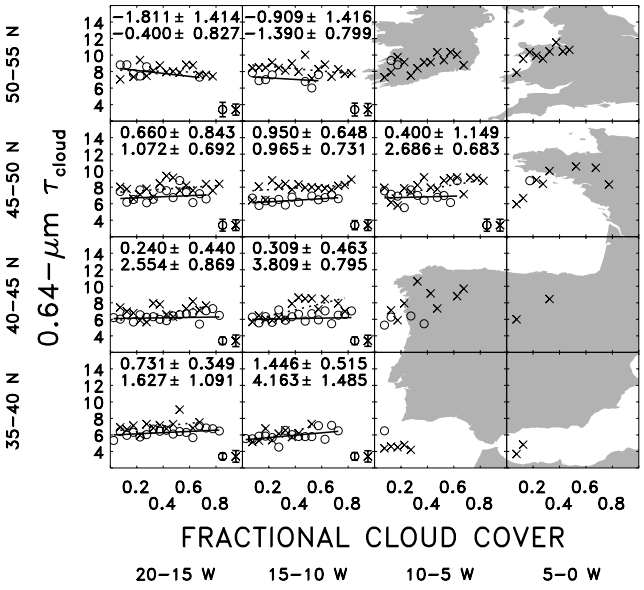

Figure 8. Same as Figure 7 but for 0.64-μm cloud optical depth.

reported that the optical depths increased with increasing fractional cloud cover. When the clouds were separated into clean and polluted clouds, the trends in cloud optical depth with increasing cloud cover became less obvious. In the nine regions with sufficient observations to calculate trends for both the clean and polluted clouds, cloud optical depths (Figure 8) for the clean clouds were relatively insensitive to fractional cloud cover in all but the southernmost regions. In six of the nine regions cloud optical depths for the polluted clouds increased as fractional cloud cover increased with the slope exceeding the estimated error in the slope. In four of these regions, the slope was twice the estimated error. Despite the trends with fractional cloud cover, clean clouds generally had smaller optical depths than their polluted counterparts. The results in Figure 8 suggest that not only were cloud optical depths sensitive to aerosol burdens, but the presence of large amounts of aerosol seemed to influence the relationship between cloud optical depth and fractional cloud cover.

[26] Despite the weak dependence of cloud optical depth on fractional cloud cover (Figure 8), liquid water path increased as fractional cloud cover increased in most regions (Figure 9). A few of the regions showed a separation in the liquid water amounts for the clean and polluted clouds, but in most regions increases in aerosol burdens had no significant impact on the relationship between cloud liquid water and fractional cloud cover. Increased aerosol burden may decrease cloud liquid water (Figure 5) but the effects of the aerosol appear to be minor compared with the changes in cloud liquid water associated with changing fractional cloud cover. As mentioned earlier, the amount of water vapor in the air mass may have a larger effect on cloud liquid water amounts than do the aerosol burdens and cloud condensation nuclei concentrations.

[27] Interestingly, column droplet concentrations decreased as fractional cloud cover increased (not shown). With the exception of one of the 5° regions, polluted clouds consistently had more cloud droplets than clean clouds. Presumably, regions with higher cloud cover fractions contained clouds that were more mature and thus allowed more time for collision-coalescence processes which may have reduced the number of droplets.

4. Radiative Forcing Estimates

[28] As was done in MCT, the response of cloud properties to changes in aerosol optical depth was used to estimate aerosol radiative forcing. In particular, estimates were made of the ratio of the aerosol indirect radiative forcing for overcast conditions to the direct radiative forcing for cloud-free conditions. These estimates facilitate comparisons with other studies [*Kaufman and Fraser*, 1997; *Sekiguchi et al.*, 2003]. In addition, comparison of the indirect radiative forcing derived from the properties of the clean and polluted clouds with that derived from the trends in cloud properties with aerosol optical depth also provide an opportunity to investigate effects that might arise from the relationships of cloud properties among themselves, such as systematic changes in droplet radius and optical depth with regional cloud cover fraction and cloud altitude as was discussed in MCT and as shown in Figures 7–9. If these relationships give rise to substantially nonlinear interactions, as might be expected from the relationships for adiabatic cloud parcel models [*Brenguier et al.*, 2000; *Szczodrak et al.*, 2001], then the aerosol indirect radiative forcing derived from the two approaches would differ. Nonetheless, as was noted in the previous section, there are processes that affect clouds and aerosols in ways that mimic the effects anticipated for the indirect effect of aerosols on clouds. Such processes like cloud contamination of the aerosol retrievals and the enhanced illumination of aerosols in the vicinity of clouds may play no role in cloud-aerosol interactions. Consequently, the results presented in this section can at best be viewed only as suggestive of the possible magnitudes given the observations and understanding that are currently available.

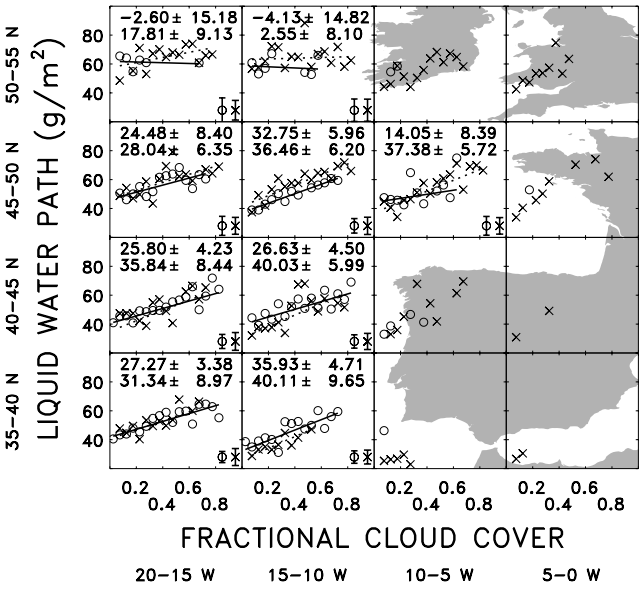

Figure 9. Same as Figure 7 but for liquid water path (g/m^2).

Table 2. Aerosol and Cloud Properties Used in Radiative Forcing Calculations Based on the Correlations With Fractional Cloud Cover (Shaded Bars in Figure 10)[a]

	20–15°W		15–10°W		10–5°W	
	Clean	Polluted	Clean	Polluted	Clean	Polluted
			50–55°N			
$\tau_{aerosol}$	0.117	0.248	0.152	0.241		
fcc	0.32	0.44	0.38	0.45		
τ_{cloud}	7.93	8.02	7.06	8.27		
R_e	11.1	11.4	11.8	11.0		
N_c	1.34	1.29	0.94	1.47		
LWP	61.1	65.2	57.3	64.1		
Z_c	1.88	1.87	1.75	1.91		
			45–50°N			
$\tau_{aerosol}$	0.105	0.230	0.105	0.241	0.104	0.256
fcc	0.38	0.45	0.39	0.40	0.36	0.41
τ_{cloud}	6.83	7.81	6.41	7.89	6.82	7.79
R_e	11.8	10.9	11.4	10.6	11.0	9.8
N_c	0.97	1.43	1.08	1.60	1.13	1.87
LWP	55.8	59.3	50.0	56.4	49.3	52.5
Z_c	1.71	1.92	1.70	1.83	1.63	1.63
			40–45°N			
$\tau_{aerosol}$	0.094	0.224	0.093	0.243		
fcc	0.36	0.42	0.34	0.38		
τ_{cloud}	6.17	6.79	6.06	7.06		
R_e	12.1	11.2	12.0	10.1		
N_c	0.94	1.34	0.98	1.57		
LWP	49.8	50.2	48.7	45.3		
Z_c	1.71	1.67	1.55	1.60		
			35–40°N			
$\tau_{aerosol}$	0.089	0.215	0.095	0.232		
fcc	0.34	0.38	0.33	0.35		
τ_{cloud}	6.23	7.05	5.86	6.29		
R_e	12.4	11.4	11.6	10.3		
N_c	0.95	1.32	0.95	1.62		
LWP	51.0	52.4	44.1	40.1		
Z_c	1.79	1.82	1.56	1.48		

[a]Properties are 0.55-μm aerosol optical depth, $\tau_{aerosol}$; fractional cloud cover, fcc; 0.64-μm cloud optical depth, τ_{cloud}; droplet effective radius, R_e (μm); column droplet concentration, N_c (10^6 cm^{-2}); liquid water path, LWP (g/m^2); and cloud altitude, Z_c (km).

[29] The radiative forcing was derived from top of the atmosphere solar radiative fluxes. As was done in MCT, these fluxes were calculated in each of the 5° regions using a broadband radiative transfer model that accounts for scattering and absorption by gases, aerosols, and clouds [*Coakley et al.*, 2002]. To estimate the aerosol direct radiative forcing for cloud-free conditions, the radiative transfer model was run twice without clouds, once with a relatively small amount of aerosol and once with a relatively large amount of aerosol. The aerosol optical depths associated with the small and large aerosol amounts were determined as follows: For the trends in cloud properties with aerosol optical depth, the small amount of aerosol was taken to have a 0.55-μm aerosol optical depth of 0.15 and the large amount of aerosol was taken to have an aerosol optical depth of 0.25. These are the same optical depths used in MCT to estimate radiative forcing. For the change in cloud properties derived from the clean and polluted clouds, the small aerosol optical depth was that associated with the average cloud fraction for the clean clouds in each of the 5° regions. These optical depths and the associated cloud properties are listed in Table 2. Likewise the large optical depth in each 5° region was that associated with the average fractional cloud cover for the polluted clouds. With no clouds, the difference in the top of the atmosphere flux of absorbed sunlight for the small and large aerosol amounts was taken to be the direct radiative forcing for cloud-free conditions. The flux calculated was the 24-hour diurnally averaged flux for 15 July which is taken to be representative of summertime conditions at the latitudes associated with each 5° region.

[30] For overcast conditions, the radiative transfer model was run twice with clouds overlying the aerosol, once with a cloud having an optical depth corresponding to that for the relatively small amount of aerosol and again for a cloud having an optical depth corresponding to the relatively large amount of aerosol. As with the estimates for the direct radiative forcing for cloud-free conditions, the small and large amounts of aerosol were taken to have 0.55-μm optical depths of 0.15 and 0.25 when the cloud properties were derived from the trends with the aerosol optical depths shown in Figures 3 and 4. When the changes in cloud properties were derived from the clean and polluted clouds, aerosol optical depths and cloud properties were those derived for the ensembles of clean and polluted clouds as listed in Table 2. Two calculations were performed for both approaches. In one, cloud liquid water was allowed to vary and the change in cloud optical depth (Figure 4 and Table 2) affected the top of the atmosphere solar radiative flux. For comparison, in the second, cloud liquid water was held constant and the observed change in droplet effective radius (Figure 3 and Table 2) was used to calculate the change in visible optical depth required to maintain constant liquid water amount. The difference in the top of the atmosphere absorbed solar radiative flux between the cases with small and large aerosol amounts were taken to be the aerosol indirect radiative forcings for overcast conditions. As was shown in MCT, the effect of the aerosol beneath the clouds on the absorbed sunlight was relatively minor compared with the effects caused by the changes in cloud optical depths. The ratios of the indirect radiative forcing for overcast conditions to the direct radiative forcing for cloud-free conditions are shown in Figure 10. Figure 10 also shows the ratios derived from the results given by MCT for the summer months of 1995.

[31] While not included in the ratios reported here, changes in cloud cover represent changes in cloud liquid water that might be attributed to the increased aerosol burden [*Ackerman et al.*, 2003]. Here the aerosol indirect radiative forcing was calculated for overcast conditions. As the results in Table 2 indicate, cloud cover increased from clean to polluted conditions for all the 5° regions. Cloud droplet effective radius and cloud optical depth for the overcast conditions were affected by changes in regional cloud cover, as shown in Figures 7 and 8 and listed in Table 2, and these effects were included.

[32] The ratios of the aerosol radiative forcings clearly vary substantially from region to region (Figure 10). First, ratios for the 5-year composite of observations in which cloud liquid water is allowed to vary (left-hand solid bars) and those for the summer of 1995 (left-hand open bars) show substantial differences, particularly in regions adjacent to land where relatively few of the observations for the 1° regions met the criteria for inclusion in the analysis. For

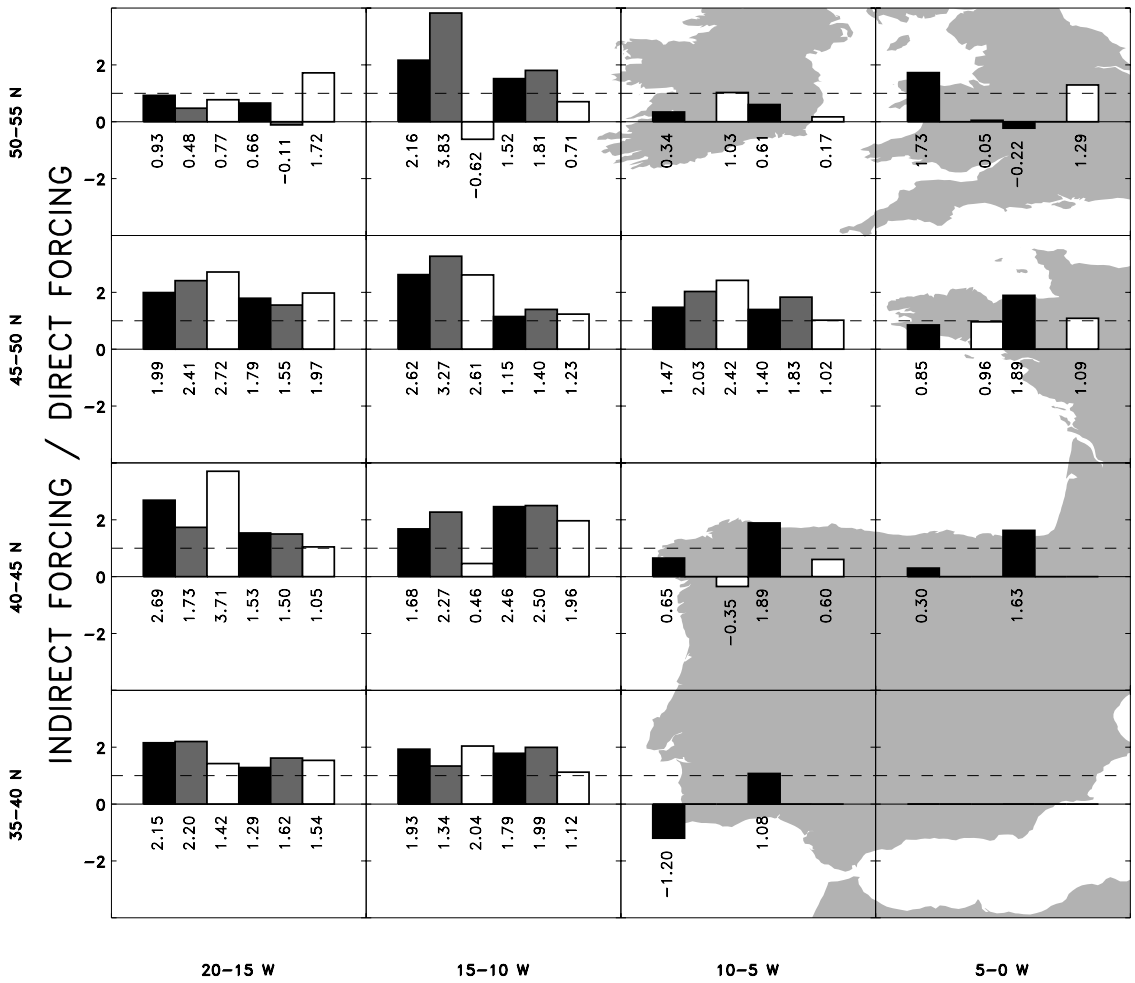

Figure 10. Ratio of aerosol indirect radiative forcing for overcast conditions to direct radiative forcing for cloud-free conditions. The three left-hand bars in each panel are based on changes in cloud optical depths. The three right-hand bars in each panel are based on changes in droplet effective radii and an assumption of fixed liquid water. The solid bars use trends in cloud properties as a function of aerosol optical depth to calculate cloud optical depth. The shaded bars are for the observations separated into clean clouds and polluted clouds and the trends in cloud properties as a function of fractional cloud cover (Figures 7 and 8). The open bars are the results of MCT based on the 1995 observations and were calculated using the same method as used for the solid bars. The dashed line represents a ratio of unity at which the aerosol indirect radiative forcing for overcast conditions equals the direct radiative forcing for cloud-free conditions.

the nine regions in which the number of cases was sufficient to estimate ratios on the basis of both the trends in the cloud properties with aerosol optical depth and the differences in cloud properties for clean and polluted clouds, the mean ratios for the 5-year composite in which cloud water was allowed to vary was 2.0, while that for 1995 was 1.7, but the root mean square (RMS) difference in the ratios was 1.2. There was somewhat better agreement between the ratios derived from the trend in cloud properties and those derived from the differences between clean and polluted clouds, for which the mean ratio was 2.2 (left-hand shaded bars) and the RMS difference in the ratios was 0.7. The relative agreement between these two estimates suggests that the trends in cloud properties with aerosol burden may, aside from the problems noted earlier, provide a suitable means for estimating the effects of aerosols on clouds. Evidently, processes that give rise to relationships such as the dependence of droplet effective radius and visible optical depth on regional cloud cover and cloud altitude, do so in ways that have little effect on the perceived response of the clouds to aerosol burdens.

[33] Compared with previous studies, MCT noted that the response of the clouds in the Amazon to smoke from clearing of the forests found by *Kaufman and Fraser* [1997] was similar to the response in the clouds for the 1995 observations. Specifically, when allowing cloud liquid water to vary, the change in albedo for overcast conditions for a given change in the 0.55-μm aerosol optical depth was found to be $\Delta r/\Delta\tau_a = 0.11$ for the 1995 observations while *Kaufman and Fraser* [1997] reported a value of 0.12 ± 0.08. Given that the ratios of the forcings for the 5-year composite were somewhat larger than that for the 1995 observations, the estimates of the increase in cloud albedo with increasing aerosol optical depth would be somewhat larger than that reported by MCT, but only by 10 − 20%, thus improving

the agreement with the *Kaufman and Fraser* [1997] results. Estimates of the aerosol direct radiative forcing reported by *Sekiguchi et al.* [2003] were consistent with that reported by MCT, but the ratio of the aerosol indirect radiative forcing for overcast conditions to the direct radiative forcing for cloud-free conditions inferred for the Sekiguchi et al. results was 3−4.5, almost twice as large as the ratio found for the 5-year composite, ∼2.

[34] Finally, when liquid water is held fixed (right-hand bars) the means of the ratios for the 5-year composite were 1.5 on the basis of the trend in cloud properties with aerosol burden, 1.6 on the basis of the differences for clean and polluted clouds, and 1.4 on the basis of the 1995 observations. Compared with the ratios obtained for varying cloud liquid water, the aerosol indirect radiative forcing for overcast conditions appears to be enhanced by 20−30% because of the changes in liquid water. Nonetheless, for the 5° regions west of the Iberian peninsula where the injection of haze from the continent and the response of the clouds is clearly evident in satellite imagery (MCT, Figure 1), cloud liquid water appears to decrease with increasing aerosol burden. In such regions, an assumption of fixed cloud liquid water would lead to an overestimate of the aerosol indirect radiative forcing for overcast conditions.

5. Conclusions

[35] Cloud and aerosol properties were retrieved in 1° × 1° latitude-longitude regions in which all the clouds were part of a single-layered, low-level system. Only regions that contained sufficient numbers of cloud-free pixels for aerosol retrievals and sufficient numbers of cloudy pixels for cloud retrievals were used in the analysis. These restrictions ensured that the clouds and the aerosols were collocated in the same region and on the same day. In addition, the focus on only low-level, single-layered maritime clouds ensured that contamination of the retrieved cloud properties by upper level or multilayered cloud systems was minimized to the extent possible with imagery data.

[36] The 1° regional means of the cloud and aerosol properties for each satellite pass were composited in the associated 5° × 5° latitude-longitude region. For each year, 1° regions were excluded if they contained means that fell outside of the 5th or 95th percentiles for the aerosol and cloud properties that fell within the 5° region. The year-to-year variations in the means and standard deviations of the cloud and aerosol properties in each 5° region were examined for the 5-year period. Annual mean aerosol optical depths decreased slowly with time. The decrease was probably the result of the precession of the satellite's orbit and consequent increase in the average solar zenith angle. The annual mean cloud properties showed no systematic variations, and changes in the annual means were often smaller than the estimated standard error in the mean and considerably smaller than the standard deviation of the overpass means within each year (Figure 1). The uniformity of the cloud and aerosol properties for all 5 years justified the combination of the observations into a single ensemble. Each satellite pass within the ensemble was taken to be an independent sample.

[37] Links between aerosol and cloud properties were analyzed in each of the 5° regions. The size of the region was chosen to minimize effects of geographic trends in the cloud and aerosol properties (Figure 2). Smaller regions would have reduced the effects of the geographic trends, but they would also have reduced the number of cases in each region thereby reducing the statistical confidence in the derived trends. The conditions of simultaneity and close spatial proximity were designed to ensure that the changes in cloud properties were probably linked to changes in aerosol burdens. The restrictions on the size of the region analyzed and on the simultaneity of the cloud and aerosol observations ensured that comparisons between clouds and aerosols on different days or in different locations were avoided. For some of the analyses, the data were segregated into clean clouds, those for which the average 0.55-μm aerosol optical depth for a 1° region was less than 0.13, the 40th percentile of the aerosol optical depths within the 20° domain for the 5-year period, and polluted clouds, those for which the average aerosol optical depth was greater than 0.17, the 60th percentile of the aerosol optical depths.

[38] The results presented here suggest that clouds are affected by increased burdens of aerosols, but they also suggest that other factors can affect the clouds and how they respond to increased aerosol burdens. As would be expected on the basis of the Twomey effect, droplet radius fell, cloud optical depth rose (Figures 3 and 4), and column droplet number concentration increased as aerosol optical depth increased. This behavior was found not only when the cloud properties were correlated with the aerosol optical depth but also when clean clouds were compared with polluted clouds (Figures 7 and 8). At the same time, droplet effective radius, cloud optical depth, and aerosol optical depth (Figure 6) all increased as the regional-scale fractional cloud cover increased. Clearly, in order to determine how aerosols affect droplet effective radius and cloud optical depth, correlations between aerosol optical depth and the cloud properties, such as shown in Figures 3−5, should be performed while holding constant the remaining cloud parameters that affect droplet radius and optical depth, such as fractional cloud cover and cloud altitude. Nonetheless, the agreement obtained between the estimates of the aerosol indirect radiative forcing derived from the trends in the cloud properties with aerosol optical depth and from the differences in the clean and polluted clouds suggests that possible nonlinear influences of regional cloud cover and cloud altitude on droplet radius and cloud optical depth appear to be minor.

[39] The tendency for both cloud and aerosol optical depths to increase as fractional cloudiness increased suggests that correlations between aerosol and cloud optical depths are not solely due to the Twomey Effect. Instead, both aerosol and cloud optical depths appear to change in response to thermodynamic fields that also affect the fractional cloud cover. Several processes, including, for example, cloud contamination in the cloud-free pixels used to determine the aerosol burdens, growth of the aerosol particles in the high relative humidity environment of the clouds, among others, were suggested as possible reasons for the increase in aerosol optical depth as cloudy pixel fraction increased. Interestingly, when polluted clouds were compared to clean clouds, the polluted clouds were more likely than clean clouds to show an increase in cloud optical depth with increasing fractional cloud cover (Figure 8). For

both polluted and clean clouds, the column droplet number concentration fell with increasing cloud cover. The fall in column droplet number concentration may reflect effects arising from collision and coalescence in the mature cloud systems that give rise to large fractional cloud cover in the 1° regions studied here.

[40] Liquid water path increased as fractional cloud cover increased (Figure 9). In some of the 5° regions, the liquid water path was largely the same for the clean and polluted clouds. In some of the regions away from the continent, the liquid water path was greater for the polluted clouds than for the clean clouds, but near the Iberian peninsula, the polluted clouds had less liquid water than the clean clouds. Evidently, clean clouds are associated with moist oceanic air and polluted clouds are associated with dry continental air. For dry conditions, liquid water path can decrease as aerosol optical depth increases [*Ackerman et al.*, 2004]. As Figure 2d appears to suggest, dry continental air is associated with small regional fractional cloud cover and moist maritime air is associated with large fractional cloud cover. Clearly, the effects of aerosols on clouds need to be disentangled from the effects of the moisture, or lack of moisture, delivered with the aerosols.

[41] Whether estimated from the trends in cloud properties with aerosol optical depth or the differences between clean and polluted clouds, the aerosol indirect radiative forcing for overcast conditions was found to be about twice as large as the corresponding aerosol direct radiative forcing for cloud-free conditions. For the forcings calculated on the basis of the clean and dirty clouds, the ratio was 2.2 with an RMS deviation of 0.9. Clearly, even within a relatively confined region and season, and even with the study limited to marine stratus and stratocumulus, the response of the clouds to changes in aerosols can differ markedly. Finally, compared with estimates based on constant cloud liquid water, the aerosol indirect radiative forcing for overcast conditions was enhanced by about 20–30% through changes in cloud liquid water. When clean and polluted clouds were separated, the average cloud cover fraction was larger for the polluted clouds than for the clean clouds. The additional cloud cover coupled with the rise in cloud optical depth with increasing regional cloud cover contributed to the enhancement in the indirect forcing that resulted from the increase in cloud liquid water.

[42] As mentioned previously, these results have to be viewed with considerable skepticism. The trends in cloud properties with aerosol optical depths could arise for reasons other than the effects of the particles on the clouds. Clearly, the underlying processes that give rise to the increase in aerosol optical depth with increasing cloud cover need to be determined. The rise in aerosol optical depth with increasing cloud cover not only affects estimates of the aerosol indirect radiative forcing, as examined here, but also estimates of the aerosol direct radiative forcing. Often estimates of the aerosol direct radiative forcing are confined to regions that are largely free of clouds, but clearly, the effects of aerosols in the vicinity of the clouds must be included, as such effects may be substantial [*Loeb and Manalo-Smith*, 2005]. Because of their different sensitivities to clouds and aerosols, combined lidar and multispectral imagery observations, as is hoped for with the suite of instruments on the A-Train upon the successful launch and operation of the CALIPSO lidar, might provide insight into the apparent increase in aerosols in the vicinity of clouds.

[43] **Acknowledgments.** This work was supported in part by the NASA CALIPSO Project through NAS1-99104, NASA grant NNG04GM11G, and by the NOAA Global Change Program through NA16GP2911. Part of this work was also performed while one of the authors (J.A.C.) was a visitor in the NASA Goddard Earth Science and Technology Fellows Program at NASA's Goddard Space Flight Center. The hospitality, suggestions, and helpfulness of colleagues at Goddard were greatly appreciated. The authors are grateful for the comments by Norman Loeb, NASA Langley Research Center, and an anonymous reviewer. The comments substantially improved the presentation of this work.

References

Ackerman, A. S., O. B. Toon, D. E. Stevens, and J. A. Coakley Jr. (2003), Enhancement of cloud cover and suppression of nocturnal drizzle in stratocumulus polluted by haze, *Geophys. Res. Lett.*, *30*(7), 1381, doi:10.1029/2002GL016634.

Ackerman, A. S., M. P. Kirkpatrick, D. E. Stevens, and O. B. Toon (2004), The impact of humidity above stratiform clouds on indirect aerosol climate forcing, *Nature*, *432*, 1014–1017.

Albrecht, B. A. (1989), Aerosols, cloud microphysics, and fractional cloudiness, *Science*, *245*, 1227–1230.

Bevington, P. R. (1969), *Data Reduction and Error Analysis for the Physical Sciences*, McGraw-Hill, New York.

Brenguier, J.-L., P. Y. Chuang, Y. Fouquart, D. W. Johnson, F. Parol, H. Pawlowska, J. Pelon, L. Schüller, F. Schröder, and J. Snider (2000), An overview of the ACE-2 CLOUDYCOLUMN closure experiment, *Tellus, Ser. B*, *52*, 815–827.

Clarke, A. D., et al. (2002), INDOEX aerosol: A comparison and summary of chemical, microphysical, and optical properties observed from land, ship, and aircraft, *J. Geophys. Res.*, *107*(D19), 8033, doi:10.1029/2001JD000572.

Coakley, J. A., Jr., W. R. Tahnk, A. Jayaraman, P. K. Quinn, C. Devaux, and D. Tanré (2002), Aerosol optical depths and direct radiative forcing for INDOEX derived from AVHRR: Theory, *J. Geophys. Res.*, *107*(D19), 8009, doi:10.1029/2000JD000182.

Coakley, J. A., Jr., M. A. Friedman, and W. R. Tahnk (2005), Retrievals of cloud properties for partly cloudy imager pixels, *J. Atmos. Oceanic Technol.*, *22*, 3–17.

Harshvardhan, S. E. Schwartz, C. M. Benkovitz, and G. Guo (2002), Aerosol influence on cloud microphysics examined by satellite measurements and chemical transport modeling, *J. Atmos. Sci.*, *59*, 714–725.

Hess, M., P. Koepke, and I. Schult (1998), Optical properties of aerosols and clouds: The software package OPAC, *Bull. Am. Meteorol. Soc.*, *79*, 831–844.

Kaufman, Y. J., and R. S. Fraser (1997), The effect of smoke particles on clouds and climate forcing, *Science*, *277*, 1636–1639.

Kaufman, Y. J., and T. Nakajima (1993), Effect of Amazon smoke on cloud microphysics and albedo—Analysis from satellite imagery, *J. Appl. Meteorol.*, *32*, 729–744.

Kidwell, K. B. (1995), NOAA Polar Orbiter data users guide, Satellite Data Serv. Div., Natl. Clim. Data Cent., Natl. Environ. Satellite, Data, and Inf. Serv., NOAA, U.S. Dep. of Commer., Washington, D. C.

Kütz, S., and R. Dubois (1997), Balloon-borne aerosol measurements in the planetary boundary layer: Particle production associated with a continental stratiform cloud, *Contrib. Atmos. Phys.*, *70*, 109–116.

Lelieveld, J., and J. Heintzenberg (1992), Sulfate cooling effect on climate through in-cloud oxidation of anthropogenic SO_2, *Science*, *258*, 117–120.

Loeb, N. G., and N. Manalo-Smith (2005), Top-of-atmosphere direct radiative effect of aerosols over global oceans from merged CERES and MODIS observations, *J. Clim.*, *18*, 3506–3526.

Lohmann, U., and G. Lesins (2002), Stronger constraints on the anthropogenic indirect aerosol effect, *Science*, *298*, 1012–1015.

Lohmann, U., J. Feichter, J. Penner, and R. Leaitch (2000), Indirect effect of sulfate and carbonaceous aerosols: A mechanistic treatment, *J. Geophys. Res.*, *105*(D10), 12,193–12,206.

Matheson, M. A., J. A. Coakley Jr., and W. R. Tahnk (2005), Aerosol and cloud property relationships for summertime stratiform clouds in the northeastern Atlantic from AVHRR observations, *J. Geophys. Res.*, *110*, D24204, doi:10.1029/2005JD006165.

Nakajima, T., A. Higurashi, K. Kawamoto, and J. E. Penner (2001), A possible correlation between satellite-derived cloud and aerosol microphysical parameters, *Geophys. Res. Lett.*, *28*, 1171–1174.

Platnick, S., and S. Twomey (1994), Determining the susceptibility of cloud albedo to changes in droplet concentration with the Advanced Very High Resolution Radiometer, *J. Appl. Meteorol.*, *33*, 334–347.

Podgorny, I. A. (2003), Three-dimensional radiative interactions in a polluted broken cloud system, *Geophys. Res. Lett.*, *30*(14), 1771, doi:10.1029/2003GL017287.

Quaas, J., O. Boucher, and F.-M. Bréon (2004), Aerosol indirect effects in POLDER satellite data and the Météorologie Dynamique—Zoom (LMDZ) general circulation model, *J. Geophys. Res.*, *109*, D08205, doi:10.1029/2003JD004317.

Seinfeld, J. H., and S. N. Pandis (1998), *Atmospheric Chemistry and Physics: From Air Pollution to Climate Change*, John Wiley, Hoboken, N. J.

Sekiguchi, M., T. Nakajima, K. Suzuki, K. Kawamoto, A. Higurashi, D. Rosenfeld, I. Sano, and S. Mukai (2003), A study of the direct and indirect effects of aerosols using global satellite data sets of aerosol and cloud parameters, *J. Geophys. Res.*, *108*(D22), 4699, doi:10.1029/2002JD003359.

Shao, H., and G. Liu (2005), Why is the satellite observed aerosol's indirect effect so variable?, *Geophys. Res. Lett.*, *32*, L15802, doi:10.1029/2005GL023260.

Stowe, L. L., H. Jacobowitz, G. Ohring, K. R. Knapp, and N. R. Nalli (2002), The Advanced Very High Resolution Radiometer (AVHRR) Pathfinder Atmosphere (PATMOS) climate dataset: Initial analyses and evaluations, *J. Clim.*, *15*, 1243–1260.

Szczodrak, M., P. H. Austin, and P. B. Krummel (2001), Variability of optical depth and effective radius in marine stratocumulus clouds, *J. Atmos. Sci.*, *58*, 2912–2926.

Tahnk, W. R., and J. A. Coakley Jr. (2001a), Improved calibration coefficients for NOAA-14 AVHRR visible and near-infrared channels, *Int. J. Remote Sens.*, *22*, 1269–1283.

Tahnk, W. R., and J. A. Coakley Jr. (2001b), Updated calibration coefficients for NOAA-14 AVHRR channels 1 and 2, *Int. J. Remote Sens.*, *22*, 3053–3057.

Twomey, S. (1974), Pollution and the planetary albedo, *Atmos. Environ.*, *8*, 1251–1256.

Wetzel, M. A., and L. L. Stowe (1999), Satellite-observed patterns in stratus microphysics, aerosol optical thickness, and shortwave radiative forcing, *J. Geophys. Res.*, *104*(D24), 31,287–31,299.

J. A. Coakley Jr. and W. R. Tahnk, College of Oceanic and Atmospheric Sciences, 104 COAS Admin Building, Oregon State University, Corvallis, OR 97331-5503, USA. (coakley@coas.oregonstate.edu)

M. A. Matheson, Department of Environmental Engineering, Building Research Institute, 1 Tehara, Tsukuba, Ibaraki, 305-0802, Japan.